

Accepted Manuscript

Title: Preparation of macroporous alginate-based aerogels for biomedical applications

Author: Marta Martins Alexandre A. Barros Sakeena Quraishi Pavel Gurikov Raman S.P. Irina Smirnova Ana Rita C. Duarte Rui L. Reis



PII: S0896-8446(15)30008-5
DOI: <http://dx.doi.org/doi:10.1016/j.supflu.2015.05.010>
Reference: SUPFLU 3330

To appear in: *J. of Supercritical Fluids*

Received date: 24-3-2015
Revised date: 14-5-2015
Accepted date: 15-5-2015

Please cite this article as: Marta Martins, Alexandre A.Barros, Sakeena Quraishi, Pavel Gurikov, S.P.Raman, Irina Smirnova, Ana Rita C.Duarte, Rui L.Reis, Preparation of macroporous alginate-based aerogels for biomedical applications, The Journal of Supercritical Fluids <http://dx.doi.org/10.1016/j.supflu.2015.05.010>

This is a PDF file of an unedited manuscript that has been accepted for publication. As a service to our customers we are providing this early version of the manuscript. The manuscript will undergo copyediting, typesetting, and review of the resulting proof before it is published in its final form. Please note that during the production process errors may be discovered which could affect the content, and all legal disclaimers that apply to the journal pertain.

Preparation of macroporous alginate-based aerogels for biomedical applications

Marta Martins^{1,2}, Alexandre A. Barros^{1,2}, Sakeena Quraishi³, Pavel Gurikov^{3*}, Raman S.P.³, Irina Smirnova³, Ana Rita C. Duarte^{1,2*}, Rui L. Reis^{1,2}

¹ 3B's Research Group - Biomaterials, Biodegradables and Biomimetics, University of Minho, Headquarters of the European Institute of Excellence on Tissue Engineering and Regenerative Medicine, AvePark, 4806-909 Taipas, Guimarães, Portugal

² ICVS/3B's - PT Government Associate Laboratory, Braga/Guimarães, Portugal

³ Hamburg University of Technology, Institute of Thermal Separation Processes, Eißendorfer Straße 38, 21073 Hamburg, Germany

*pavel.gurikov@tuhh.de; Tel: +49 40 42878 4275, fax: +49 40 42878 4072

Highlights

- alginate-starch Ca-crosslinked aerogels by CO₂ induced gelation and sc-drying;
- macroporosity due to CO₂ expansion and intrinsically high mesoporosity;
- alginate-starch aerogels are bioactive and non-cytotoxic.

ABSTRACT

Aerogels are a special class of ultra-light porous materials with growing interest in biomedical applications due to their open pore structure and high surface area. However, they usually lack macroporosity, while mesoporosity is typically high. In this work, carbon dioxide induced gelation followed by expansion of the dissolved CO₂ was performed to produce hybrid calcium-crosslinked alginate-starch hydrogels with dual meso- and macroporosity. The hydrogels were subjected to solvent exchange and supercritical drying to obtain aerogels. Significant increase in macroporosity from 2 to 25 % was achieved by increasing expansion rate from 0.1 to 30 bar/min with retaining mesoporosity (BET surface and BJH pore volume in the range 183 – 544 m²/g and 2.0 – 6.8 cm³/g, respectively). *In vitro* bioactivity studies showed that the alginate-starch aerogels are bioactive, *i.e.* they form hydroxyapatite crystals when immersed in a simulated body fluid solution. Bioactivity is attributed to the presence of calcium in the matrix. The assessment of the biological performance showed that the aerogels do not present a cytotoxic effect and the cells are able to colonize and grow on their surface. Results presented in this work provide a good indication of the potential of the alginate-starch aerogels in biomedical applications, particularly for bone regeneration.

KEYWORDS

aerogels, alginate, starch, tissue engineering, supercritical fluids, CO₂ induced gelation

INTRODUCTION

An ideal scaffold for tissue engineering must meet particular requirements to achieve the desired biological response: the scaffold should possess inter-connecting pores of appropriate size to favor tissue integration and vascularization, be made from material with controlled biodegradability, have appropriate surface chemistry to favor cellular attachment, differentiation and proliferation, possess adequate mechanical properties to match the intended site of implantation and handling, should not induce any adverse response and be easily fabricated into a variety of shapes and sizes [1]. Some attempts have recently been made to address tissue engineering and regenerative medicine (TERM) problems using aerogels as scaffolds. Aerogels are well known ultra-light highly porous materials with an open structure, large specific surface area and pore volume. High mesoporosity comparable to the native extracellular matrix (*ca.* 80% porosity) is favorable condition for cell growth, making aerogels an ideal candidate for a number of biomedical applications, including tissue engineering. Nevertheless, macroporosity of these structures should be improved to promote cell migration into the matrices and enhance mass transfer between the scaffold and the bulk phase.

The fact that biopolymers can be used for aerogel production was recognized by Samuel Kistler as far back as in 1931. He demonstrated for the first time the possibility to prepare aerogels from polysaccharides (gelatin, agar, nitrocellulose and cellulose) opening up the challenge to extend this research with the statement “we see no reason why this list may be not extended indefinitely” [2]. Since then, the aerogel production has been growing from different biopolymer-based precursors [3].

Up to now, few biopolymer-based aerogels have been assessed for TERM applications. Silva and co-workers have reported processing of chitin aerogels as tissue engineering scaffolds [4–7]. In these works chitin has been modified to render a bioactive material. Aerogel processing has also been changed to induce higher porosity into the matrices. Preparation of chitosan aerogels and their *in vitro* assessment has also been reported [8,9].

Among others, alginate and starch are polysaccharides, which are widely adopted in several fields (pharmacy, cosmetics, medicine, agriculture and biotechnology). Due to their non-cytotoxicity, stability, availability, renewability and well-studied gelation chemistry [10], they are attractive candidates for aerogel production [3]. Further diversity in the aerogel functionality can be achieved in hybrid systems. In recent times, hybrid aerogels, *i.e.* composed of two or more chemically or physically bound components, have been attracting considerable attention. The main advantage of these materials is that they inherit the intrinsic properties of aerogels with improved and tunable mechanical properties, wettability and chemical functionality [11]. For instance, materials based on pure alginate often have high hydrophilicity and insufficient mechanical properties [12]. In order to extend the range of potential applications, some approaches have been developed for alginate modification including extra crosslinking [13] or by incorporation of reinforcing components [12,14,15]. Recently we presented a study of hybrid alginate-lignin aerogels and demonstrated that are non-cytotoxic and feature good cell adhesion [16]. In this work, we have further explored the preparation of hybrid alginate aerogels with starch as the second component and evaluated these aerogels as 3D constructs for TERM applications.

2. MATERIALS AND METHODS

2.1 Materials

The polymers employed in this study were sodium alginate (Sigma Life science, Germany) and pea starch with amylose content of 35 % (Roquette, France). Light precipitated calcium carbonate (Ph. Eur. grade) was donated by Magnesia GmbH (Germany). Anhydrous ethanol (99.9 %) used in the solvent exchange step was purchased from H. Möller GmbH & Co.KG (Germany). Food grade carbon dioxide used for drying was obtained from AGA Gas GmbH (Germany). *In vitro* cell culture and bioactivity studies were performed with chemicals of analytical reagent or tissue culture grade.

2.2 Aerogel preparation

Hybrid alginate-starch aerogels were prepared similarly to previously described alginate-lignin aerogels [16]. Starch (ST) was dispersed in hot water (80 °C) under continuous stirring and cooled to room temperature. 3 wt% starch solution was mixed with 3 wt% sodium alginate (Na-Alg) to obtain a target Na-Alg : ST ratio (1:1, 2:1 or 5:1, w/w). Calcium carbonate was used as crosslinker. CaCO₃ to Na-Alg ratio was varied at two levels, 1.82 and 3.64 mmol/g, denoted as $q = 1$ and $q = 2$, respectively. The mixture was homogenized for 1 min using Ultra-turrax (IKA, Staufen, Germany).

To prepare hydrogels, homogenized mixtures were treated with pressurized gaseous carbon dioxide at 50 ± 5 bar and room temperature for various time intervals (3 – 48 h) in a high pressure autoclave [17]. To introduce macroporosity, the autoclave was depressurized at three rates, 0.1 10 or 30 bar/min, denoted in the following as slow (SD), normal (ND) and fast (FD) depressurization, respectively. Linear dimensions of the hydrogels were measured with a caliper to quantify syneresis during the gelation. Hydrogels were washed with water and underwent a stepwise solvent exchange procedure with different grades of ethanol (30, 60, 90 and twice 100 wt% ethanol/water mixtures were used, 24 h each step).

Alcogels were placed into the high pressure autoclave (preheated to 40 °C). Carbon dioxide was pumped into the autoclave to reach 120 bar to ensure conditions above critical pressure and temperature of CO₂/ethanol mixture of any composition. Drying was performed for 4 h with CO₂ flow rate of *ca.* 60 g/h. The processing steps involved in the preparation of alginate-starch aerogel scaffolds are depicted in Fig. 1.

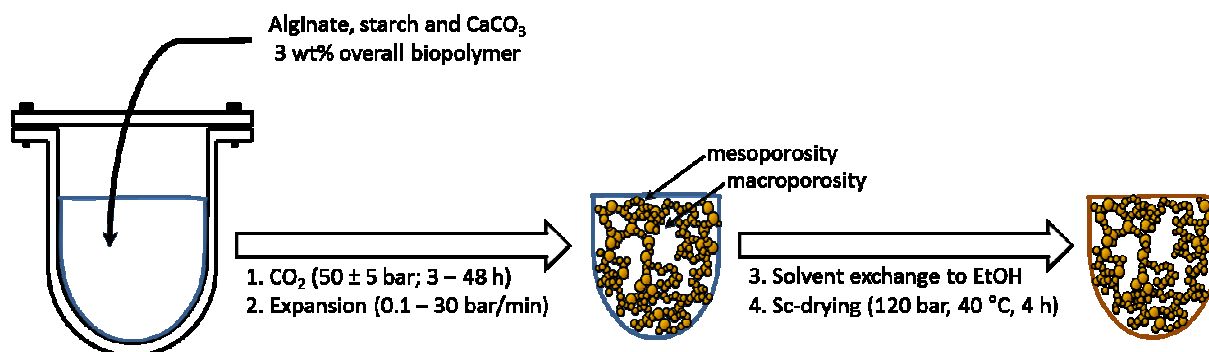


Figure 1. Schematic representation of the alginate-starch aerogel processing

2.3 Morphological characterization

Cylindrical samples of the aerogels were used to calculate the apparent density as the ratio between the weight and the volume (measured with a caliper). The weight was measured after degassing (<1 mPa, 75 °C, 24 h). The same degassing conditions were employed to measure BET specific surface area and BJH specific pore volume using low temperature N₂ adsorption-desorption analysis (Nova 3000e, Quantachrome Instruments).

The aerogel matrixes were observed by Leica Cambridge S360 Scanning Electron Microscope (SEM). Cross sections of the specimens were examined after fracturing in liquid nitrogen. The matrices were fixed by mutual conductive adhesive tape on aluminum stubs and covered with gold palladium using a sputter coater.

The morphological structure at macroporous level was evaluated by micro-computed tomography (micro-CT) using Scanco 20 equipment (Skyscan 1702, Belgium) with penetrative X-rays of 30 keV and 167 μA, in high resolution mode with a pixel size of 14 μm and 1.5 s of exposure time. A CT analyzer (v1.5.1.5, SkyScan) was used to calculate the parameters from 2D images of the aerogels.

2.4 Mechanical tests

Compressive analyses of the aerogel scaffolds were measured using INSTRON 5540 (Instron Int. Ltd, High Wycombe, UK) universal testing machine with a load cell of 1 kN. Compression testing was carried out a crosshead speed of 2 mm/min, until a maximum deformation of 60 %. The compressive modulus (E) is defined as the initial linear modulus on the stress/strain curves. The results are presented as the mean of three experiments ± standard deviation. In wet state, the samples were immersed for 5 – 10 min in PBS solution (pH 7.4) before compression tests.

2.5 *In vitro* studies

2.5.1 Water uptake

The swelling capability of the matrices prepared was assessed after 1, 3, 7 and 14 days. The samples were immersed in 5 mL of a Tris-HCl solution with pH 7.4 and placed in a water bath at 37 °C under 60 rpm. The weight of the swollen samples was measured after removing excess of surface fluid with filter paper. For each time point the water uptake value, WU , was determined from the weight of the swollen sample (m_t) and the initial weight (m_0) as follows:

$$WU = \frac{m_t - m_0}{m_0} \times 100\%.$$

2.5.2 Bioactivity evaluation

In vitro bioactivity tests were carried out by soaking alginate-starch aerogel samples in 5 mL of simulated body fluid (SBF) at 37 °C at pH 7.45 within 14 days. The SBF was prepared following the protocol described by Kokubo and Takadama [18]. All ingredients (NaCl, NaHCO₃, KCl, K₂HPO₄·3H₂O, MgCl₂·6H₂O, CaCl₂, Na₂SO₄, C₄H₁₁NO₃ and HCl) were purchased from Sigma-Aldrich. After 0, 1, 7 and 14 days the SBF was removed using filter paper, the samples were rinsed with distilled water, dehydrated in ethanol and dried in a critical point dryer. The dried samples were analyzed by SEM, FTIR spectroscopy, Energy Dispersive Spectroscopy (EDS) and X-ray diffraction (XRD). SEM was performed as described above (Section 2.3). The appearance of the calcium phosphate layer on the surface

of the matrices after immersion in SBF solution was observed by a Leica Cambridge S360 equipped with an energy dispersive spectrometer.

FTIR analysis was performed for both original and immersed in SBF solution samples. Infrared spectra were recorded with a Shimadzu-IR Prestige 21 spectrometer in the spectral region of $4000 - 400 \text{ cm}^{-1}$ with resolution of 2 cm^{-1} at 32 scans. The samples were powdered, mixed with KBr and processed into pellets. XRD measurements were performed for the original aerogels after 14 days of immersion. A Bruker D8 Discover X-ray diffractometer was operated at 40 kV and 40 mA using Cu K α radiation. The detector was scanned over a range of 2θ angles from 15 to 60° at a step size of 0.04° and dwell time of 1 s per step.

2.5.3 *In vitro* cell culture studies

Cell seeding and culture. A mouse fibroblast-like cell line (L929 cell line, European Collection of Cell Cultures, UK) at a concentration 1×10^5 cells/mL was seeded on alginate-starch aerogel matrices and cultured for 1, 3 and 7 days. Triplicates were used for each time point. The cell-material constructs were maintained in Dulbecco's modified Eagle's medium (DMEM, Sigma-Aldrich, Germany) supplemented with 10% heat-inactivated fetal bovine serum (Biochrom AG, Germany) and 1% antibiotic-antimycotic solution (Gibco, UK) and incubated at 37°C in a 5% CO_2 atmosphere. Before cell seeding the structures were immersed in sterile PBS for one hour in order to swell the matrix.

Cell adhesion and morphology. To evaluate the cell morphology, the cells-scaffold constructs were fixed with 4% formalin (Sigma-Aldrich, Germany) for 15 min and then washed with PBS. Afterwards, scaffolds are dehydrated through a graded series of ethanol and dried supercritically. Finally, they were sputter-coated and analyzed by SEM as described above.

Cell viability. The metabolic activity of the cells seeded on the samples was accessed by Alamar Blue assay (BFU012B, Arium). This assay is based on the quantitative metabolic transformation of blue non-fluorescent resazurin to pink fluorescent resofurin by living cells. The samples were incubated in a 10% of Alamar Blue in a basal medium at 37°C , 5% CO_2 for 4 h. The fluorescence of the supernatant solution was read at 570/600 nm excitation/emission on a multiwell microplate reader (Synergy HT, Bio-Tek Instruments). The samples were analyzed in triplicate and the results are presented as the mean of at least three measurements \pm standard deviation.

2.6 Statistical analysis

Statistical analysis of the data was conducted using IBM SPSS Statistics version 20 software. Shapiro-Wilk test was employed to evaluate the normality of the data sets. Once the results obtained do not follow a normal distribution, non-parametric tests, in particular Kruskal-Wallis test, were used to infer statistical significant differences. Differences between the groups with $p < 0.05$ were considered to be statistically significant.

3. RESULTS AND DISCUSSION

3.1 Textural and mechanical properties

Aerogels processing starts with the formation of the hydrogels in aqueous medium. In this work the crosslinking of alginate-starch blends was induced by treatment with pressurized carbon dioxide [16,19]. This method is a variation of the internal gelation method [20] and

relies on the liberation of calcium cation from insoluble calcium carbonate triggered by pH lowering in CO₂/water system. Usage of pressurized carbon dioxide for gelation of other biopolymers [21–23] and inorganic systems [24,25] has been reported in the literature.

The gelation process is followed by depressurization and solvent exchange. In this work we studied the influence of the depressurization rate on macroporosity of the samples and performed the solvent exchange as consecutive step.

In the preliminary experiments it was observed that soft hydrogels can be damaged at high depressurization rate. Thus, stiffness of hydrogels is an important parameter for fast depressurization. As it is known from the literature, there are three methods for improving the stiffness of alginate-based hydrogels: increasing the crosslinking degree [26], reinforcement with a second component [12,15] and syneresis (aging). The latter process consists at macrolevel in decrease of the hydrogel volume with time along with increase of the stiffness [27]. At microlevel both egg-box dimerization and further intra-cluster association [28] cause network densification and thus syneresis.

Syneresis S was quantified by measuring diameter of the hydrogel D_t after a given time t relative to the diameter of the gelation mold D_0 and expressed as $S = 100\% \times D_t/D_0$. It was observed that syneresis develops with time reaching more than 30 % after 48 h (Fig. 2). Hydrogels, which underwent the 24 h syneresis, were stiff enough to withstand the highest pressure expansion rate (30 bar/min). Thus, duration of exposure to CO₂ was fixed at 24 h in all further experiments.

To convert hydrogels into aerogels, carbon dioxide induced gelation and depressurization was followed by water removal process, namely solvent exchange. This step is to ensure that less than 2 wt% water is present in the gel before supercritical carbon dioxide drying (sc-drying). During the solvent exchange gels experience certain degree of shrinkage. Intensity of the solvent exchange is found to be crucial as it determines the overall shrinkage and thus to what extent existing nano- and mesoporous structure is preserved [3]. Multistep solvent exchange to ethanol was used in this study as it allows to keep the overall linear shrinkage at level of 5 – 20%. Obtained alcogels were dried in mild conditions at 120 bar and 40 °C using supercritical carbon dioxide above critical pressure of the ethanol/CO₂ mixture [29] to preserve mesoporous structure of the wet gel in the dry form.

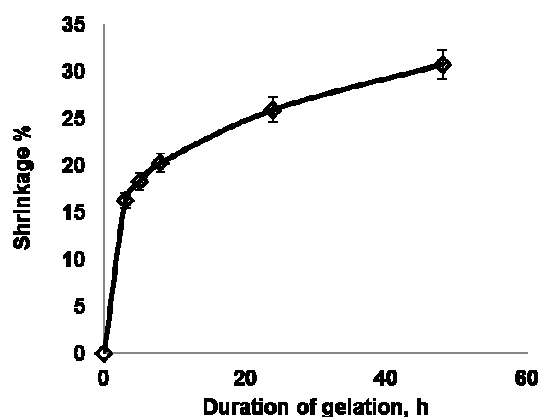


Figure 2. Syneresis as a function of gelation time for the sample AS-SD, Na-Alg : ST = 1:1 (w/w), $q = 2$.

Previous studies have reported that the textural, mechanical, water uptake and drug release properties of the alginate-based materials can be influenced by the composition of the alginate (*i.e.* molecular weight, G/M ratio) and the second component [12,30,31] as well as degree of crosslinking [15]. To reveal the influence of the compositions and crosslinking degree (q) on the textural properties of the alginate-starch aerogels, apparent density was first measured (Fig. 3A). As all formulations were of the same overall biopolymer content (3 wt%), apparent density can be viewed as a measure of the hydrogel rigidity (resistance against solvent exchange and sc-drying). As it follows from Fig. 3A, aerogel density is approximately constant (0.06 g/cm^3) for alginate-to-starch ratios of 2:1 and 5:1 regardless of crosslinking degree. Since starch cannot participate in the formation of egg-box junctions, it is expected that larger starch content (1 : 1 ratio) would lead to the dilution of the system and may potentially interrupt the formation of the stable gel network. Indeed, 30% increase in apparent density was observed at 1:1 (w/w) alginate-to-starch ratio and $q = 1$. This behavior can be however reverted at $q = 2$ (Fig. 3A).

It is known that pure alginate aerogels usually have superior textural properties than starch counterparts [3]. So it was expected that surface area and pore volume may diminish as starch content increases. Indeed, a monotonic decrease in surface area and pore volume were observed at higher starch content and $q = 2$ (Fig. 3B and C). Values at $q = 1$ are generally lower and show a maximum for 2 : 1 alginate-to-starch ratio. Nevertheless, obtained BET surface area and BJH pore volume clearly indicate that all samples have well-developed mesoporous structure. In search of a compromise between possibly high starch content, low density, high surface area and pore volume, the formulation with alginate-to-starch ratio of 1:1 (w/w) and $q = 2$ was selected for further *in vitro* studies. This formulation had density of 0.048 g/cm^3 , surface area of $272 \text{ m}^2/\text{g}$ and pore volume of $2.4 \text{ cm}^3/\text{g}$.

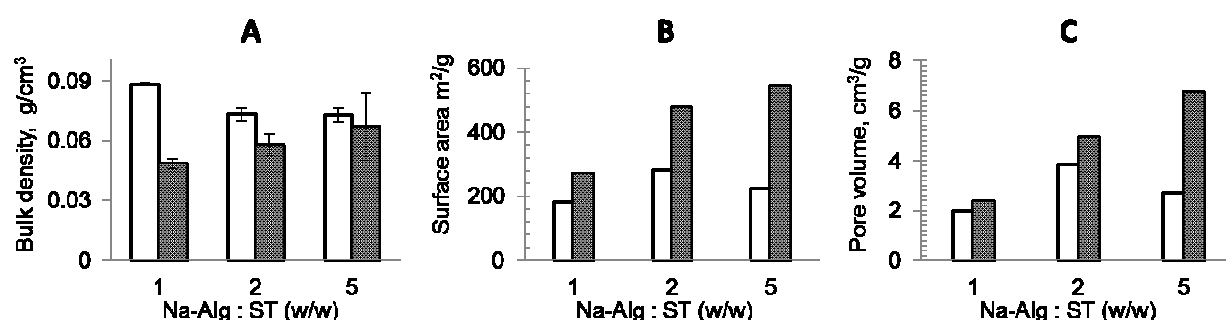


Figure 3. Bulk density (A), specific surface (B) and pore volume (C) of alginate-starch aerogels (AS-SD) at two crosslinking degree $q = 1$ (white bars) and $q = 2$ (shaded bars).

Aerogels produced at slow depressurization rate showed almost no macroporosity detectable by micro-CT (pore size less than $15 - 20 \mu\text{m}$). However, as it follows from the specific volume (reciprocal density) all samples have significant fraction (54 – 88 %) of the pores in the range of $150 \text{ nm} - 15 \mu\text{m}$, which cannot be attributed to BJH volume. These pores however are too small to allow cell penetration and migration. Due to this fact macroporosity was introduced into hydrogels by gas expansion after 24 h of gelation time. Visual assessment of the foamed hydrogels (ND and FD) revealed cavities of several millimeters in sizes,

whereas hydrogels obtained at 0.1 bar/min were macroscopically homogeneous. Results of the micro-CT and SEM analysis are shown in Fig. 4 and summarized in Table 1.

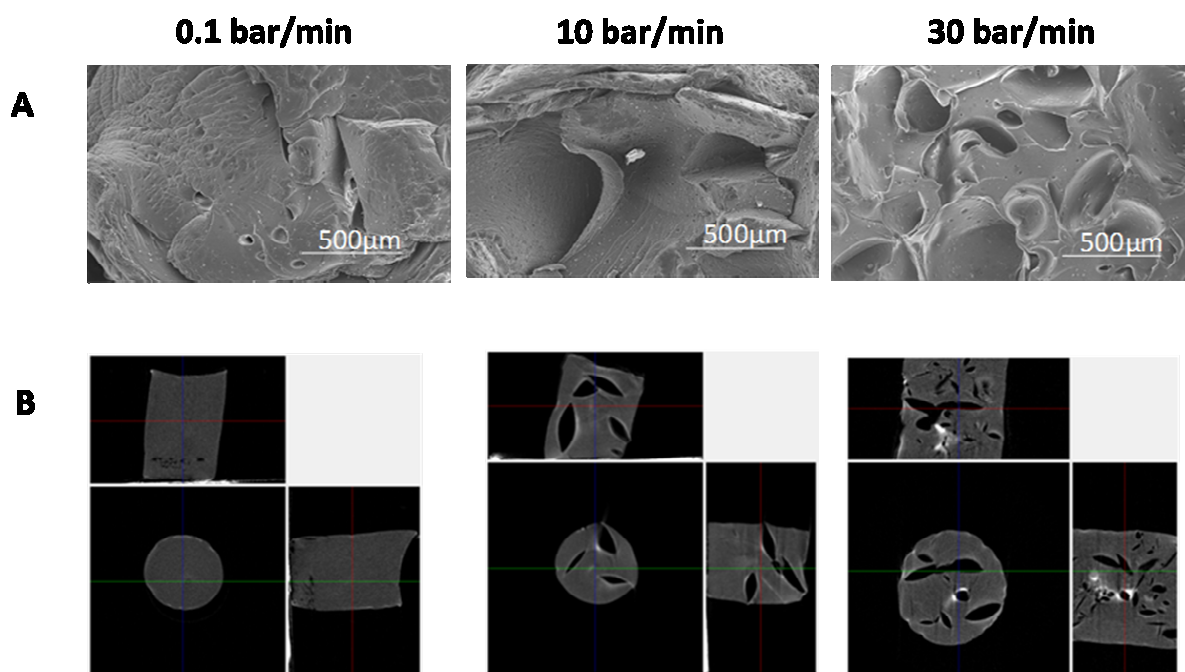


Figure 4. SEM micrographs (A) and micro-CT 2D images (B) of alginate-starch aerogels processed at different rates of CO₂ depressurization; Na-Alg : ST = 1:1 (w/w), $q = 2$.

The SEM images presented in Fig. 4 show the change in porosity when the depressurization rate is increased. More clear trend was observed by micro-CT analysis, which also allows the visualization of the three axis of symmetry of the sample. Further, from image analysis of the micro-CT scans it is possible to quantify the morphological parameters which characterize the structures, such as porosity, mean pore size and interconnectivity (Table 1). Significant increase in porosity from 2% up to 25% was achieved by increasing the depressurization rate. These observations were coupled with an increase in the mean pore size and interconnectivity, revealing that macroporosity was introduced by the fast expansion of CO₂ after gelation. In the context of tissue engineering applications, the morphological parameters obtained for the ND and FD samples meet the requirements requested for tissue engineering scaffolds. Karageorgiou and Kaplan have reviewed the influence of porosity and pore size on the formation of new bone and concluded that 100 μm pore size corresponds to the minimum pore size required for cell migration and penetration into the bulk of the structure as well as for nutrients diffusion into the bulk and waste out of the matrix [32]. The results obtained for the alginate-starch aerogels are above this range being good candidates for future developments in the field.

The mechanical properties of the matrices are another characteristic that needs to be determined to evaluate the feasibility for TERM applications. Different tissues present different mechanical properties and it is important to ensure that the scaffold is able to withstand the mechanical properties and load-bearing of the site of defect. Furthermore, biomedical implants are normally applied in hydrated environments, thus it is more relevant to determine the properties in the wet state. The mechanical response of the matrices prepared at different rates of depressurization was evaluated in compression mode and the values of elastic modulus, namely, Young's modulus (E) of these structures, in both dry and wet state are shown in Table 1.

The results suggest that Young's modulus is affected by the depressurization rate. We observed an increase in the modulus with increase in depressurization rate. The same tendency was observed in the wet state, but the values were lower by a factor of 10. In the previous study on alginate-lignin aerogels, we found lower Young's modulus for aerogels with higher macroporosity [16]. Results in Table 1 show the opposite tendency. Increase in stiffness along with increase in pore size has been reported in the literature [33]. Current experimental data is not sufficient to draw a consistent conclusion on reasons underlying this phenomenon.

The Young's modulus of the dry aerogels are comparable with porous chitin matrices produced by Silva and co-workers [7]. Wet aerogels show E values in the range of extensively studied chitosan hydrogels, which were also processed in pressurized carbon dioxide [34]. It is expected that in an *in vivo* situation, the stiffness increases due to the formation of a mineral layer and the cell extracellular matrix.

3.2 Water uptake, bioactivity and cell studies

It has been described that water uptake is an important parameter in the characterization of biodegradable polymers, which affects the degradation profile and swelling, induces changes in mechanical properties and influences the biological response [25]. It has been shown for alginate-based drug delivery systems that pure calcium-crosslinked alginate is permeable to water and has fast water uptake. Blending with other polymers is one approach to control the drug release from alginate formulations [12]. For tissue engineering applications, it would be beneficial to abate the scaffold degradation and to match it with the rate of new bone tissue regeneration. Addition of more hydrophobic starch was aimed to decrease water uptake rate. Preliminary study was performed on the aerogels with alginate-to-starch ratio of 1:1, 2:1 and 5:1 (w/w) at $q = 1$ and 2, which were depressurized at 30 bar/min. The aerogels were immersed in Tris-HCl buffer (pH 7.4, room temperature) for 60 s and weight increase was recorded. Previously selected formulation with Na-Alg : ST ratio of 1:1 and $q = 2$ showed lowest water uptake of $106 \pm 28 \%$, whereas formulations with higher alginate content demonstrated uptake in the range of 150 – 200 %. This finding further supports that the formulation Na-Alg : ST = 1:1, $q = 2$ is feasible for further assessment in terms of water uptake. The water uptake of this formulation was investigated for a period up to 14 days in Tris-HCl at 37 °C (Fig. 5). Tris-HCl buffer was chosen instead of commonly used PBS due to its lower affinity to calcium ions. Phosphate ions present in PBS leads to fast dissolution of the alginate materials so that water uptake may be distorted due to fast calcium leakage (see [16] for further discussion).

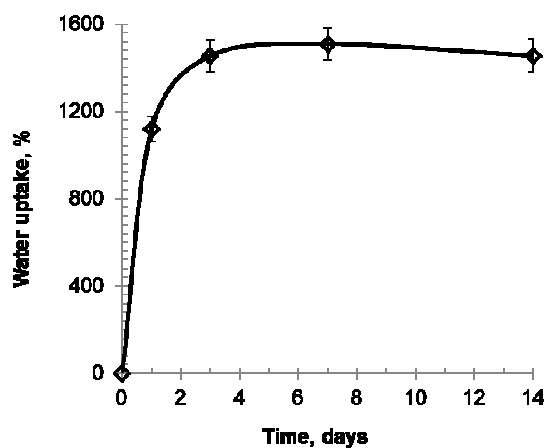


Figure 5. Water uptake profile of AS-FD with alginate-to-starch ratio of 1:1 (w/w) and $q = 2$ as a function of immersion time in Tris-HCl solution at 37 °C and 60 rpm.

Equilibrium water uptake of 1454 % was reached in 3 days with slight degradation after 2 weeks. Alginate-based materials presented in the literature show water uptake in the wide range from 30 to 35 000% [35–37] making direct comparison difficult. Obtained result is comparable with alginate-lignin aerogel reported in our previous work [16].

According to Kokubo and Takadama's the definition of bioactivity refers to a bioactive material as a material on which bone-like hydroxyapatite will form selectively after immersion in a simulated body fluid [18]. Polymers are usually inert materials which lack bioactivity and unable to induce mineral deposition at the surface. One way to overcome this drawback is to develop composite materials containing bioglasses or bioactive ceramics, which are able to induce the precipitation of hydroxyapatite crystals and the formation of a calcium phosphate layer similar to bone [38–40]. The formation of this layer enhances the integration of the scaffold on the defect site by promoting bone bonding to the material. Marine corals mostly constituted by calcium carbonate have been reported in the literature to be interesting alternatives to conventional bioceramics [41,42]. Other authors have also reported the use of calcium carbonate, *e.g.* Matsuya and coworkers described CaCO_3 as one of the materials that can form a chemical bond with bone *in vivo* [43]. Combes *et al.* have reported the application of calcium carbonate as good bone cement candidate [44].

In this work we hypothesize that simultaneous presence of calcium cations within the alginate matrix and CO_3^{2-} and PO_4^{3-} in SBF solution could cause at neutral pH the precipitation of calcium carbonate and phosphates on the surface and thus promote the bioactivity of the aerogel. *In vitro* bioactivity tests carried out in simulated body fluid confirmed our hypothesis.

The bioactive character of alginate-starch aerogels, in particular, AS-FD was tested *in vitro* by analyzing the hydroxyapatite formation at the surface after exposure to SBF solution, which has ion concentrations nearly equal to human blood plasma. SEM micrographs of the scaffolds after 1, 7 and 14 days of immersion in SFB are shown in Figure 6.

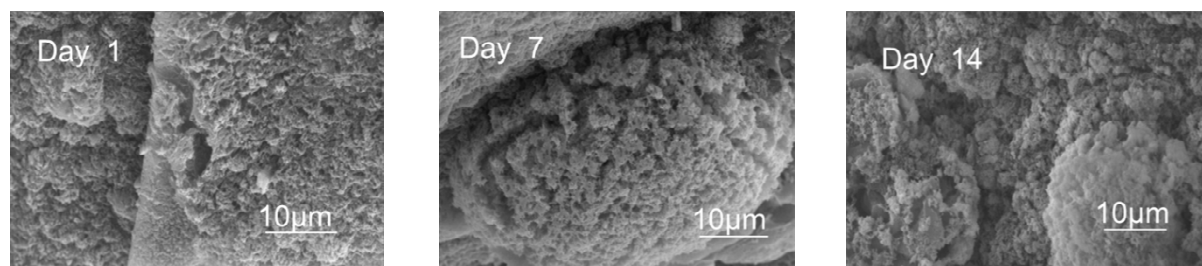


Figure 6. SEM images of surface of the scaffolds prepared (AS-FD) immersed for different periods in SBF solution.

The SEM images show the deposition of crystals on the surface of the matrices immediately after one day of immersion in SBF. After 14 days, most of the surface is covered with calcium phosphate crystals, as proven after chemical analysis performed by EDS (Fig. 7).

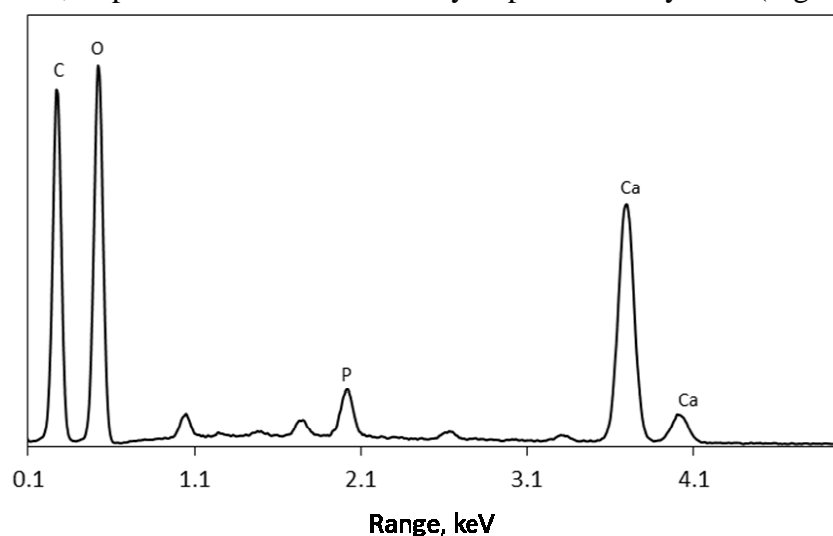


Figure 7. EDS spectrum of the alginate-starch aerogel scaffolds (AS-FD) after 14 days immersion in SBF.

The morphological and chemical analysis obtained by SEM-EDS was complemented by FTIR and XRD. Calcium phosphate layer was further characterized to identify the characteristic crystalline peaks. Fig. 8 shows the FTIR and XRD spectra of the samples before and after 14 days of immersion.

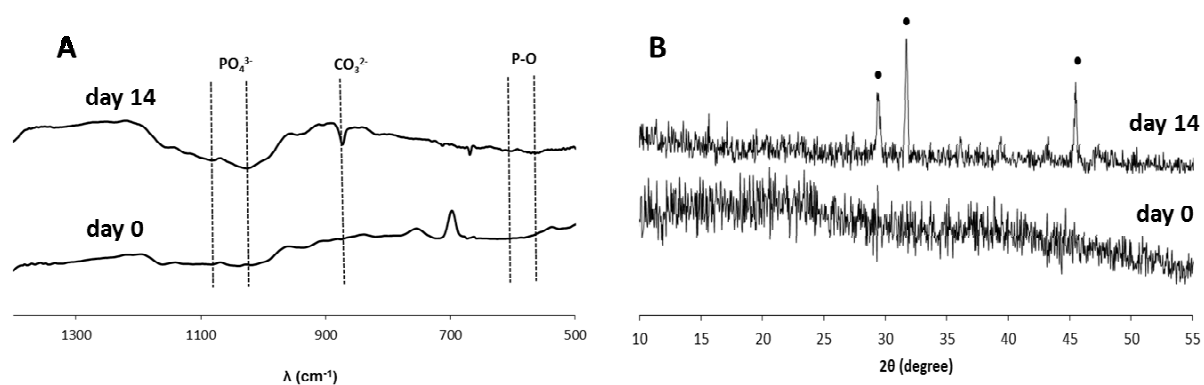


Figure 8. FTIR (A) and XRD (B) spectra of the aerogels (AS-FD) immersed in SBF solution for 14 days and original aerogels (day 0).

Characteristic peak of the phosphate (PO_4^{3-}) groups at 1020 cm^{-1} and 1080 cm^{-1} and absorption peak of carbonate groups at 878 cm^{-1} were detected [45]. Moreover, it was possible visualize at 570 and 600 cm^{-1} two peaks characteristic of the P–O bond [46]. This result indicates that alginate-starch aerogel is a bioactive material, being able to form hydroxyapatite crystals when immersed in simulated body fluid solution. XRD analysis confirmed the presence of the main characteristic peak of hydroxyapatite (2,1,1) at $2\theta = 32^\circ$, an indication that an apatite-like phase formed upon immersion exhibits the typical features of the carbonated apatite found in bone [18]. Another two high intensity peaks located at $2\theta = 29^\circ$ and $2\theta = 45^\circ$ (contribution of (0,0,2) and (2,2,2) reflection planes) were detected (ASTM JCPDS 9-432). The XRD data was in good agreement with FTIR analysis and demonstrated that hydroxyapatite was formed on the aerogel scaffolds. These results provide strong indication that the aerogels are indeed bioactive and are able to induce the precipitation of hydroxyapatite on the surface. This finding further supports the feasibility of these materials for bone tissue engineering applications.

The assessment of the biocompatibility of novel materials requires the screening of eventual cytotoxicity and cellular response. This was carried out through *in vitro* tests using a fibroblast-like cell line. The viability of the cells after 1, 3 and 7 days is presented in Fig. 9.

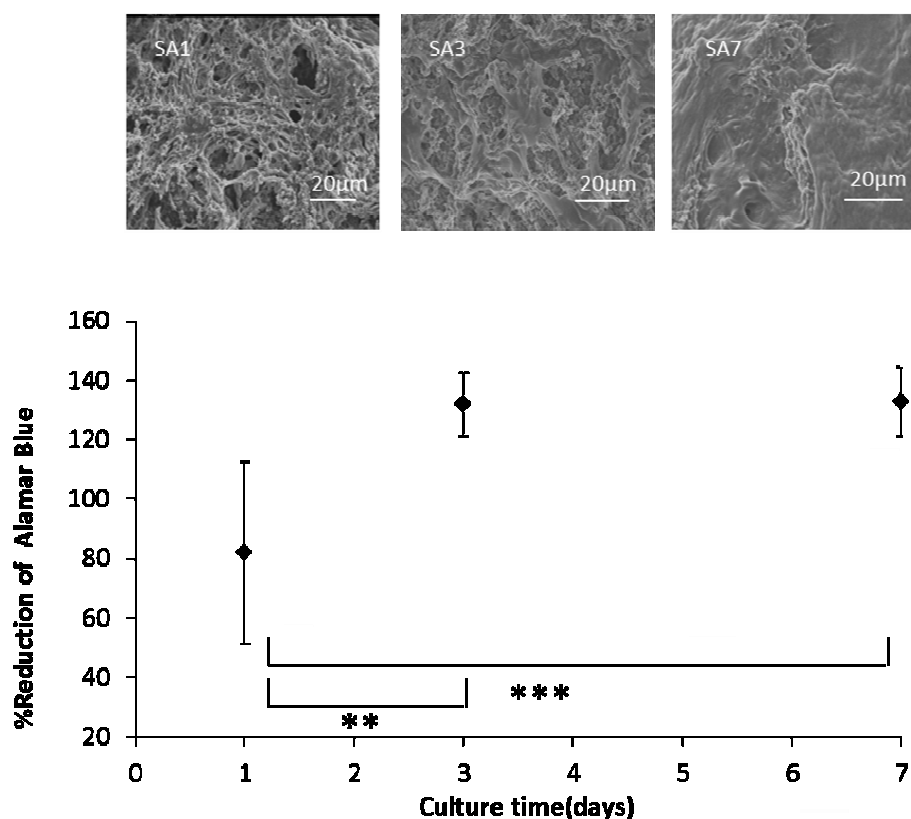


Figure 9. Reduction of alamarBlue (%) as a function of culture time coupled with SEM images of cells cultured *in vitro* on the surface of AS-FD scaffold.

The alamarBlue assay revealed that the L929 cells were metabolically active on alginate-starch aerogels over the culture period under study, and there was a significant increase after 3 days of culture time in comparison with day 1 (Fig. 9). This effect was however not as great from day 3 to day 7, but the viability of the cells is not compromised when in contact with the

developed aerogels. SEM analysis to the surface of the cultured materials was carried out. The images obtained and presented in Fig 9, show different morphologies to the seeded surface over different periods of culture time which means the cells were able to adhere and proliferate on these matrices. In first image is possible to visualize well the roughness of the matrix compared with the last image where the surface is almost covered by a cell layer.

CONCLUSION

Hybrid alginate-starch aerogels were prepared by four step procedure, which involves gelation of the alginate-starch blend in pressurized carbon dioxide, expansion of CO₂, solvent exchange and supercritical drying. Expansion step is aimed to introduce macroporosity into aerogels. The textural analysis by nitrogen adsorption and SEM revealed that aerogels are both meso- and macroporous. Macroporosity is found to be highly dependent on the depressurization rate of the system. The morphological analysis obtained by scanning electron microscopy and micro-CT revealed high interconnectivity and pore size above 100 μm. Mechanical tests demonstrated an increment of Young's modulus for aerogels with higher macroporosity. In terms of swelling capability, alginate-starch aerogels showed sufficient water uptake up to *ca.* 1500 %. *In vitro* tests revealed that aerogels are bioactive, non-cytotoxicity and the cells are able to adhere and proliferate on surface of the scaffolds. Obtained results suggest that alginate-starch aerogels are good candidates for biomedical applications, in particular, bone tissue engineering.

ACKNOWLEDGMENTS

The research leading to these results has received funding from Fundação da Ciência e Tecnologia (FCT) through the project ENIGMA – PTDC/EQU-EPR/121491/2010, from the European Union's Seventh Framework Programme (FP7/2007-2013) under grant agreement no. REGPOT-CT2012-316331-POLARIS and from the project “Novel smart and biomimetic materials for innovative regenerative medicine approaches (ref.: RL1 – ABMR – NORTE-01-0124-FEDER-000016)” cofinanced by North Portugal Regional Operational Programme (ON.2-O Novo Norte), under the National Strategic Reference Framework (NSRF), through the European Regional Development Fund (ERDF) and FEDER.

Marta Martins is grateful for financial support from Fundação da Ciência e Tecnologia (FCT) through the grant BIM/PTDC/EQU-EPR/121491/2010/ENIGMA. Bilateral 3B's Research Group and TUHH cooperation project FCT-DAAD 57036335 and DFG project SM82/8-2 are gratefully acknowledged.

References

- [1] W. Liu, Y. Cao, Application of scaffold materials in tissue reconstruction in immunocompetent mammals: Our experience and future requirements, *Biomaterials* 28 (2007) 5078–5086.
- [2] S.S. Kistler, Coherent Expanded Aerogels and Jellies, *Nature* 127 (1931) 741.
- [3] C.A. García-González, M. Alnaief, I. Smirnova, Polysaccharide-based aerogels— Promising biodegradable carriers for drug delivery systems, *Carbohydrate Polymers* 86 (2011) 1425–1438.

- [4] S.S. Silva, A.R.C. Duarte, J.M. Oliveira, J.F. Mano, R.L. Reis, Alternative methodology for chitin–hydroxyapatite composites using ionic liquids and supercritical fluid technology, *Journal of Bioactive and Compatible Polymers* 28 (2013) 481–491.
- [5] S.S. Silva, A.R.C. Duarte, J.F. Mano, R.L. Reis, Design and functionalization of chitin-based microsphere scaffolds, *Green Chemistry* 15 (2013) 3252–3258.
- [6] S.S. Silva, A.R.C. Duarte, J.F. Mano, R.L. Reis, A particle-agglomeration method for the preparation of 3D chitin-based hybrid matrices, *Journal of Tissue Engineering and Regenerative Medicine* 6 (2012) 186–186.
- [7] S.S. Silva, A.R.C. Duarte, A.P. Carvalho, J.F. Mano, R.L. Reis, Green processing of porous chitin structures for biomedical applications combining ionic liquids and supercritical fluid technology, *Acta Biomaterialia* 7 (2011) 1166–1172.
- [8] S. Cardea, P. Pisanti, E. Reverchon, Generation of chitosan nanoporous structures for tissue engineering applications using a supercritical fluid assisted process, *The Journal of Supercritical Fluids* 54 (2010) 290–295.
- [9] R. Kumari, P.K. Dutta, Physicochemical and biological activity study of genipin-crosslinked chitosan scaffolds prepared by using supercritical carbon dioxide for tissue engineering applications, *International Journal of Biological Macromolecules* 46 (2010) 261–266.
- [10] P.B. Malafaya, G.A. Silva, R.L. Reis, Natural–origin polymers as carriers and scaffolds for biomolecules and cell delivery in tissue engineering applications, *Advanced Drug Delivery Reviews* 59 (2007) 207–233.
- [11] H. Ramadan, T. Coradin, S. Masse, H. El-Rassy, Synthesis and Characterization of Mesoporous Hybrid Silica-Polyacrylamide Aerogels and Xerogels, *Silicon* 3 (2010) 63–75.
- [12] C.M. Silva, A.J. Ribeiro, D. Ferreira, F. Veiga, Insulin encapsulation in reinforced alginate microspheres prepared by internal gelation, *European Journal of Pharmaceutical Sciences* 29 (2006) 148–159.
- [13] S.N. Pawar, K.J. Edgar, Alginate derivatization: A review of chemistry, properties and applications, *Biomaterials* 33 (2012) 3279–3305.
- [14] Y. Cheng, L. Lu, W. Zhang, J. Shi, Y. Cao, Reinforced low density alginate-based aerogels: Preparation, hydrophobic modification and characterization, *Carbohydrate Polymers* 88 (2012) 1093–1099.
- [15] J. Sun, H. Tan, Alginate-Based Biomaterials for Regenerative Medicine Applications, *Materials* 6 (2013) 1285–1309.
- [16] S. Quraishi, M. Martins, A.A. Barros, P. Gurikov, S.P. Raman, I. Smirnova, et al., Novel non-cytotoxic alginate–lignin hybrid aerogels as scaffolds for tissue engineering, *The Journal of Supercritical Fluids* (2015), DOI: 10.1016/j.supflu.2014.12.026, in press.
- [17] I. Smirnova, J. Mamic, W. Arlt, Adsorption of drugs on silica aerogels, *Langmuir* 19 (2003) 8521–8525.
- [18] T. Kokubo, H. Takadama, How useful is SBF in predicting in vivo bone bioactivity?, *Biomaterials* 27 (2006) 2907–2915.
- [19] P. Gurikov, S.P. Raman, D. Weinrich, M. Fricke, I. Smirnova, A novel approach to alginate aerogels: carbon dioxide induced gelation, *RSC Advances* 5 (2015) 7812–7818.
- [20] K.Y. Lee, D.J. Mooney, Alginate: Properties and biomedical applications, *Progress in Polymer Science* 37 (2012) 106–126.
- [21] M.L. Floren, S. Spilimbergo, A. Motta, C. Migliaresi, Carbon Dioxide Induced Silk Protein Gelation for Biomedical Applications, *Biomacromolecules* 13 (2012) 2060–2072.
- [22] S.P. Raman, P. Gurikov, I. Smirnova, Hybrid alginate based aerogels by carbon dioxide induced gelation: novel technique for multiple applications, Submitted to *The Journal of Supercritical Fluids* (2015).

- [23] R.R. Mallepally, M.A. Marin, M.A. McHugh, CO₂-assisted synthesis of silk fibroin hydrogels and aerogels, *Acta Biomaterialia* 10 (2014) 4419–4424.
- [24] I. Smirnova, W. Arlt, Synthesis of Silica Aerogels: Influence of the Supercritical CO₂ on the Sol-Gel Process, *Journal of Sol-Gel Science and Technology* 28 (2003) 175–184.
- [25] B. Zhu, W. Wei, G. Ma, Y. Zhuang, J. Liu, L. Song, et al., A pressurized carbonation sol-gel process for preparing large pore volume silica and its performance as a flattening agent and an adsorbent, *The Journal of Supercritical Fluids* 97 (2015) 1–5.
- [26] C.K. Kuo, P.X. Ma, Ionically crosslinked alginate hydrogels as scaffolds for tissue engineering: Part 1. Structure, gelation rate and mechanical properties, *Biomaterials* 22 (2001) 511–521.
- [27] K.I. Draget, O. Gåserød, I. Aune, P.O. Andersen, B. Storbakken, B.T. Stokke, et al., Effects of molecular weight and elastic segment flexibility on syneresis in Ca-alginate gels, *Food Hydrocolloids* 15 (2001) 485–490.
- [28] Y. Fang, S. Al-Assaf, G.O. Phillips, K. Nishinari, T. Funami, P.A. Williams, et al., Multiple Steps and Critical Behaviors of the Binding of Calcium to Alginate, *The Journal of Physical Chemistry B* 111 (2007) 2456–2462.
- [29] C.-Y. Day, C.J. Chang, C.-Y. Chen, Phase equilibrium of ethanol + CO₂ and acetone + CO₂ at elevated pressures, *Journal of Chemical & Engineering Data* 41 (1996) 839–843.
- [30] A. López-Córdoba, L. Deladino, M. Martino, Release of yerba mate antioxidants from corn starch-alginate capsules as affected by structure, *Carbohydrate Polymers* 99 (2014) 150–157.
- [31] J. Malakar, A.K. Nayak, A. Das, Modified starch (cationized)-alginate beads containing aceclofenac: Formulation optimization using central composite design, *Starch - Stärke* 65 (2013) 603–612.
- [32] V. Karageorgiou, D. Kaplan, Porosity of 3D biomaterial scaffolds and osteogenesis, *Biomaterials* 26 (2005) 5474–5491.
- [33] A.N. Stachowiak, A. Bershteyn, E. Tzatzalos, D.J. Irvine, Bioactive Hydrogels with an Ordered Cellular Structure Combine Interconnected Macroporosity and Robust Mechanical Properties, *Advanced Materials* 17 (2005) 399–403.
- [34] C. Ji, N. Annabi, A. Khademhosseini, F. Dehghani, Fabrication of porous chitosan scaffolds for soft tissue engineering using dense gas CO₂, *Acta Biomaterialia* 7 (2011) 1653–1664.
- [35] S.K. Bajpai, R. Tankhiwale, Investigation of water uptake behavior and stability of calcium alginate/chitosan bi-polymeric beads: Part-1, *Reactive and Functional Polymers* 66 (2006) 645–658.
- [36] A.R. Kulkarni, K.S. Soppimath, T.M. Aminabhavi, A.M. Dave, M.H. Mehta, Glutaraldehyde crosslinked sodium alginate beads containing liquid pesticide for soil application, *Journal of Controlled Release* 63 (2000) 97–105.
- [37] Y.S. Choi, S.R. Hong, Y.M. Lee, K.W. Song, M.H. Park, Y.S. Nam, Study on gelatin-containing artificial skin: I. Preparation and characteristics of novel gelatin-alginate sponge, *Biomaterials* 20 (1999) 409–417.
- [38] G. Kaur, O. P. Pandey, K. Singh, D. Homa, B. Scott, G. Pickrell, A review of bioactive glasses: Their structure, properties, fabrication and apatite formation, *Journal of Biomedical Materials Research Part A* 102 (2014) 254–274.
- [39] A. Hoppe, V. Mouriño, A.R. Boccaccini, Therapeutic inorganic ions in bioactive glasses to enhance bone formation and beyond, *Biomaterials Science* 1 (2013) 254–256.
- [40] K. Rezwani, Q.Z. Chen, J.J. Blaker, A.R. Boccaccini, Biodegradable and bioactive porous polymer/inorganic composite scaffolds for bone tissue engineering, *Biomaterials* 27 (2006) 3413–3431.
- [41] G. Guillemin, J.-L. Patat, J. Fournie, M. Chetail, The use of coral as a bone graft substitute, *Journal of Biomedical Materials Research* 21 (1987) 557–567.

- [42] H. Ohgushi, M. Okumura, T. Yoshikawa, K. Inboue, N. Senpuku, S. Tamai, et al., Bone formation process in porous calcium carbonate and hydroxyapatite, *Journal of Biomedical Materials Research* 26 (1992) 885–895.
- [43] S. Matsuya, X. Lin, K. Udoh, M. Nakagawa, R. Shimogoryo, Y. Terada, et al., Fabrication of porous low crystalline calcite block by carbonation of calcium hydroxide compact, *Journal of Materials Science: Materials in Medicine* 18 (2007) 1361–1367.
- [44] C. Combes, B. Miao, R. Bareille, C. Rey, Preparation, physical–chemical characterisation and cytocompatibility of calcium carbonate cements, *Biomaterials* 27 (2006) 1945–1954.
- [45] H.R. Ramay, M. Zhang, Preparation of porous hydroxyapatite scaffolds by combination of the gel-casting and polymer sponge methods, *Biomaterials* 24 (2003) 3293–3302.
- [46] J. Ma, C.Z. Chen, D.G. Wang, X.G. Meng, J.Z. Shi, In vitro degradability and bioactivity of mesoporous CaO-MgO-P₂O₅-SiO₂ glasses synthesized by sol–gel method, *Journal of Sol-Gel Science and Technology* 54 (2010) 69–76.

Table 1: Morphological characteristics determined by micro-CT and mechanical properties of the alginate hybrid materials.

Rate of depressurization, bar/min	Morphological parameters			Mechanical properties
	Porosity %	Mean pore size (μm)	Interconnectivity (%)	$E(\text{MPa})$
0.1	2.3 \pm 0.1	-	-	0.52 \pm 0.07 ^d 0.06 \pm 0.01 ^w
10	14 \pm 0.5	255 \pm 9	44 \pm 2	0.73 \pm 0.14 ^d 0.04 \pm 0.01 ^w
30	25 \pm 2	431 \pm 158	66 \pm 17	1.35 \pm 0.21 ^d 0.12 \pm 0.14 ^w